1	The Pliocene-to-present course of the Tennessee River
2	Short title: Pliocene-to-present course of the Tennessee River
3	
4	William E. Odom ¹ , Darryl E. Granger ²
5	
6	¹ U.S. Geological Survey, Florence Bascom Geoscience Center, 12201 Sunrise Valley Dr., MS
7	926A, Reston, VA 20192
8	² Department of Earth, Atmospheric, and Planetary Sciences, Purdue University, 550 Stadium
9	Mall Dr., West Lafayette, IN 47907
10	
11	Corresponding author: William Odom (wodom@usgs.gov)
12	
13	
14	
15	
16	
17	
18	
19	
20	
21	
22	
23	

Abstract

The Tennessee River, a primary drainage of the southern Appalachians and significant sediment source for the Gulf of Mexico, is generally considered to be the product of captures that rerouted the river from a more direct gulfward course. Sedimentary and genetic evidence indicate a paleo-Tennessee flowed into the Mobile Basin through the Late Miocene, although alternate models propose other redirections of the river. We constrain the river course's age by dating terraces near Pickwick, Tennessee with cosmogenic ²⁶Al/¹⁰Be isochron burial dating. We find that the river's present path dates to at least the Early Pliocene.

The Tennessee River watershed

The Tennessee River follows an unusually indirect path (Figure 1), turning away from its eventual outlet in the Gulf of Mexico to flow across more resistant rocks in several locations. In discussions ranging over a century, these turns have been attributed to ancient antecedent drainage patterns (e.g., Milici 1968) or recent capture (e.g., Hayes and Campbell 1894). We provide a minimum age for the present-day course of the Tennessee River by dating a series of terraces near Pickwick, Tennessee, and extrapolate incision rates to suggest the river was captured into its northern course away from the Gulf of Mexico by the Early Pliocene.

Flowing from its headwaters in the Blue Ridge Mountains of the southern Appalachians, where it picks up a distinctive quartzite bedload (Mills and Kaye 2001), the Tennessee River follows the southwestern strike of the Valley and Ridge for >200 km before turning west and cutting into the Cumberland Plateau through the meandering 300 m-deep Walden Gorge near Chattanooga, Tennessee. The river then skirts the Nashville Dome on a topographic surface

developed atop the resistant Mississippian Fort Payne Chert. It cuts through the Fort Payne Chert at a ~50 m high knickzone at Muscle Shoals, Alabama that marks its most significant convexity (Figure 1) and soon encounters weakly consolidated Cretaceous to Paleogene Coastal Plain sediments in the Mississippi Embayment near Pickwick, Tennessee. Rather than continue west to the Mississippi River through the more erodible younger rocks, it turns northward and flows away from the Gulf of Mexico and diametrically opposed to the Mississippi River <200 km to the west. After joining the Ohio River, the river executes a hairpin bend to join the Mississippi River, ultimately draining to the Gulf of Mexico. Why and when the Tennessee River turns north at Pickwick instead of cutting across the highly erodible Coastal Plain sediments remains an open question, primarily due to a lack of datable terraces.

Evidence of a more direct route to the Gulf of Mexico comes from Late Cretaceous to Eocene fluvial sediments and basin-floor deposits near Mobile, Alabama (Blum et al. 2017), as well as Grenville (1300-950 Ma) and Appalachian-Ouachita (500-280 Ma) detrital zircon U-Pb age signatures in terrestrial Miocene outcrops attributed to an ancestral Tennessee River (Xu et al. 2017). High sedimentation rates near Mobile Bay in the Early Pliocene (Galloway et al., 2011; Snedden et al., 2018) have been interpreted as evidence for uplift and erosion of the southern Appalachians (Gallen et al. 2013; Xu et al. 2017); however, various age estimates for the capture of the Tennessee River to the north range from Eocene to Oligocene (Blum et al. 2017) to Pliocene (Snedden and Galloway, 2019).

Additional evidence for a former connection to the Gulf of Mexico comes from comparisons of the modern Tennessee River's aquatic species with those in rivers draining to Mobile Bay. Hayes and Campbell (1894) first suggested a link based on geomorphic reconstructions and the distribution of molluscs, though Johnson (1905) pointed out that

molluscs could have been carried on the feet of birds. More recently, Mayden (1988) and Hoagstrom et al. (2014) examined the similarities of fish species across the southeastern United States and found that the Mobile Basin shows among the fewest affinities with other rivers. They interpreted that the Tennessee River may have once been connected to Mobile Bay, well prior to the Pleistocene. Near and Keck (2005) used a DNA-based molecular clock from related darter species in the Tennessee and Mobile systems to estimate that a former connection was broken at 9.0 ± 1.7 Ma. Kozak et al. (2006) dated divergence of salamander species from the Upper Tennessee River and Mobile Basin to ~4 Ma for the sister clades of *Eurycea cirrigera* and *E. wilderae*, and ~7 Ma for the sister clades of *E. junaluska* and *E. aquatica*. Together with the marked decrease in sediment delivery to Mobile Bay near that time, the genetic evidence points to separation of the Tennessee River and Mobile Basin in the Late Miocene to Early Pliocene.

The earliest sedimentary evidence for a northward-flowing river comes from the Upland Complex gravels that are widely distributed across western Kentucky (Potter 1955). The Upland Complex is likely time-transgressive, but several locations have recently been dated to the Middle Pliocene or older (Odom et al. 2020). A better constraint on the river's northward route, however, comes from a set of well-developed but previously undated terraces near its northward bend at Pickwick.

Site descriptions

At its northward turn near Pickwick, Tennessee, the Tennessee River departs the Mississippian limestones and flows across a dissected zone of poorly consolidated Cretaceous to Paleogene sand and gravel of the Mississippi Embayment. A sequence of terraces has been carved into the erodible rock (Parks and Russell 1975). Self (2003) mapped these terraces and

divided them into five levels, with bases ranging in elevation from 128-213 m above sea level (asl) (Figure 1).

The highest terrace, Nt₅, has a strath elevation of 117 m above the bedrock channel and is the most quartzite-rich deposit, comprised of 84% rounded quartzite clasts. This terrace contains no chert, indicating that the upstream Fort Payne Chert had not been breached by the time of its deposition (Self 2003). All of the lower terraces (Nt₁- Nt₄) contain abundant chert, indicating that the Tennessee River began incising through the Fort Payne Chert sometime between the deposition of Nt₅ and Nt₄, which has a strath elevation of 87 m above the bedrock channel (Self 2003). The thickness of the terraces varies significantly between different levels; our observations ranged from 0.5 m in Nt₄ to 6-10 m in the lowest three terraces (Nt₁- Nt₃). Higher terraces are generally more dissected; examination in the field revealed scant evidence of Nt₅, while Nt₄ is substantially eroded and insufficiently thick for cosmogenic nuclide burial dating. We sampled terrace levels Nt₁- Nt₃ for ²⁶Al/¹⁰Be isochron burial dating. Sample locations are provided in Table 1. At each site, we collected quartzite cobbles for ²⁶Al/¹⁰Be burial isochrons and sand for determination of paleo-erosion rates.

Methods

The isochron burial dating method uses the relative radioactive decay of ²⁶Al and ¹⁰Be in quartz that was exposed at the ground surface and then buried. For quartz that was originally derived from a steadily eroding landscape, the ²⁶Al and ¹⁰Be concentrations after burial can be closely approximated by equation (1):

114
$$N_{26} = \left(\frac{P_{26}}{P_{10}}\right) \frac{N_{10} - N_{10,pb}}{1 + \frac{N_{10}}{P_{10}\tau_{10}}} e^{-t/\tau_{bur}} + N_{26,pb}$$
 (1)

Where N_{26} and N_{10} are the respective concentrations of 26 Al and 10 Be (at/g), P_{26}/P_{10} is the production rate ratio in the sediment source area, taken as 6.8 (Caffee et al. 2017), $N_{26,pb}$ and $N_{10,pb}$ are the respective concentrations of 26 Al and 10 Be produced after burial (at/g), τ_{26} and τ_{10} are the mean-lives, taken as 1.02 My for 26 Al (Nishiizumi 2004) and 2.005 My for 10 Be (Chmeleff et al. 2010; Korschinek et al. 2010), t is the burial age, and $\tau_{bur} = (\tau_{26}^{-1} - \tau_{10}^{-1})^{-1}$ (yr). Solution of equation (1) requires additional knowledge of postburial production rates. Assuming a constant postburial production rate ($P_{i,pb}$), the ratio $P_{26,pb}/P_{10,pb}$ can be obtained from Balco (2017), here taken as 8.3, to calculate the ratio $N_{26,pb}/N_{10,pb}$.

A suite of samples collected at the same depth but with different inheritances will form a gentle curve on a plot of ²⁶Al vs. ¹⁰Be, with slope dependent on the burial age and the intercept dependent on postburial production. All samples that share a single burial episode should lie along a single isochron. However, terraces of large rivers or those that are incising into terraces upstream may have clasts with prior burial histories (Wittmann et al. 2011). These clasts will lie below the isochron, reflecting their previous burial. Unless such clasts are identified and removed from the fit, they will increase scatter in the isochron and will bias the result toward an excessively old age. Reworked clasts can often be identified by significantly lower ²⁶Al/¹⁰Be ratios relative to other isochron measurements, which cause them to fall below the line defined by equation 1.

To identify reworked clasts, we evaluate the isochron fit using the mean squared weighted deviation (MSWD). Samples with a high weighted deviation are excluded following a modified Chauvenet's criterion. If any sample has a weighted deviation of more than two standard errors (p < 0.05), then the sample with the highest misfit is removed from the isochron.

This process is repeated until either the MSWD indicates a sufficiently good fit, or until all samples lie within two standard errors of the isochron.

Results

Burial isochrons for the three terraces yield ages spanning the Pliocene (Figure 2, Tables 1-3). The highest dated terrace, Nt₃, with a strath at 168 m and a tread at 179 m, dates to 4.43 \pm 0.92 Ma (MSWD = 2.0). Below it, the Nt₂ terrace, with a strath at 154 m and a tread at 166 m, yields a burial age of 2.83 \pm 0.31 Ma (MSWD = 2.4) after excluding one reworked clast. The lowest dated terrace, Nt₁ with a strath at 139 m and a tread at 147 m, initially yielded a burial age of 2.94 \pm 0.16 Ma (MSWD = 4.3) after excluding reworked clast PW4-4. Removal of clast PW4-18 substantially improves the MSWD and yields a slightly younger age of 2.69 \pm 0.18 Ma (MSWD = 3.3), which we prefer. The uncertainties reported above are analytical error only. Incorporating uncertainties in mean lives (2% for ²⁶Al and 1% for ¹⁰Be) and production rate ratio (3%) marginally increases overall age uncertainties (4.46 \pm 0.97 Ma for Nt₃, 2.85 \pm 0.33 Ma for Nt₂, and 2.71 \pm 0.21 Ma for Nt₁).

Discussion

Our isochron burial ages for the terraces of the lower Tennessee River provide new constraints on its course. The 4.43 ± 0.92 Ma age of Nt₃ demonstrates that the Tennessee River has flowed north from Pickwick, Tennessee since at least the Early Pliocene. However, the presence of higher terraces implies a longer history. We can estimate the ages of the higher terraces by extrapolating the river incision rate. The strath of Nt₃ is at 168 m asl, while the strath of terrace Nt₂ is at 154 m asl; their difference in ages yields an incision rate of 8.8 ± 5.4 m/My.

Assuming a uniform incision rate and extrapolating to the highest terrace Nt_5 implies a possible age range of 16.5-6.2 Ma (Figure 3). While this age range is highly approximate, it is consistent with biological evidence for the Tennessee River's capture to its present configuration in the Late Miocene. Remarkably, the extrapolated age of the highest terrace agrees closely with the 9.0 ± 1.7 Ma age inferred from DNA dating of vicariance of darters (Near and Keck 2005), and matches the \sim 7 Ma age estimated from salamander DNA (Kozak et al. 2006). Deep water basin fan sedimentation records favor a slightly younger redirection of the Tennessee River, likely during the Early Pliocene (Snedden and Galloway, 2019). Taken together, the faunal and sedimentary data provide independent evidence for redirection sometime during the Late Miocene to Early Pliocene.

The history of incision and aggradation following deposition of the Nt₁ terrace remains undated. The bedrock valley of the Tennessee River is presently filled with ~15 m of sediment deposited after the local 'deep stage,' when the river incised to its deepest level. Future work dating the valley fill could clarify the timing of deep stage incision and subsequent aggradation. Cosmogenic ²⁶Al/¹⁰Be burial dating of cave sediments along the Cumberland and Green Rivers, which also drain to the lower Ohio River, has shown rapid entrenchment near 2.0 and 1.5 Ma, respectively, followed by regional aggradation near 0.8 Ma (Granger et al. 2001; Anthony and Granger 2006). The lower Tennessee River likely responded similarly, with deep stage incision in the Early Pleistocene and aggradation associated with the Middle Pleistocene transition. In contrast to regional incision on these other rivers, however, any Pleistocene incision pulse on the Tennessee River has not propagated upstream of the resistant Muscle Shoals knickpoint. Consequently, the Tennessee River has few terraces upstream of its major knickpoint and its caves show no evidence of rapid base level lowering.

If the Tennessee River flowed directly to the Gulf of Mexico until at least the Late Miocene, where was the capture point? One commonly proposed capture point is where the river exits the Valley and Ridge at Walden Gorge. Hayes and Campbell (1894) proposed that the paleo-Tennessee River had previously continued down strike, flowing southwestward from Chattanooga via the Coosa River (Figure 1). Recent geomorphic modeling by Gallen (2018) rejuvenated this hypothesis by showing that knickzones in the upper Tennessee River basin are consistent with a pulse of incision driven by capture at Walden Gorge in the Miocene. However, there are no known gravels in the area of the proposed Coosa-Tennessee linkage (Mills et al. 2005; Persons 2010). Based on the distribution of vein quartz pebbles in Cretaceous conglomerates, which would have been sourced from the Appalachian Mountains, Adams (1928) suggested that the Tennessee River has flowed west across Walden Ridge since the Cretaceous and that the meandering gorge was superposed from that time.

Another possible drainage capture point is where the Tennessee River turns north at Pickwick, Tennessee, to follow the strike of the Cretaceous sediments. Self (2003) mapped quartz gravels and hypothesized that the Tennessee River continued west to the Mississippi River through the Hatchie River valley until the Late Miocene-Early Pliocene, although the quartz could have been reworked from Cretaceous gravels in the watershed (Parks 1992), and a course through the Hatchie River would not connect to Mobile Bay. Mills and Kaye (2001) found several areas with scattered high-level quartz pebbles indicating possible connections between the Tennessee River and the Mobile Basin, notably along the Sipsey, Black Warrior, and Tombigbee Rivers, but there is little clear evidence of a major channel, and the Tombigbee gravels are reworked from Cretaceous deposits (Russell and Schmitz 2003). Alternatively,

and that no major connections existed between the Tennessee and Mobile River basins. Given the poor preservation of fluvial deposits (Mills and Kaye 2001), the location of the former connection remains ambiguous.

CONCLUSIONS

The course of the Tennessee River exerted primary controls on fan deposition in the Gulf of Mexico, faunal distribution, landscape evolution, and sediment transport in the southern Appalachian Mountains throughout the Neogene. Previous reconstructions of the river's history have been difficult to test due to limited age control. Our ²⁶Al/¹⁰Be isochron ages for the terraces near Pickwick, Tennessee show that the river has existed in its modern configuration since at least the Early Pliocene, consistent with DNA evidence for darter and salamander vicariance (Near and Keck 2005; Kozak et al. 2006) and reduced sediment delivery to the Gulf of Mexico in the Early Pliocene (Snedden and Galloway, 2019).

ACKNOWLEDGMENTS

This work was supported by National Science Foundation EAR1700821 to D. Granger. We thank Arthur Merschat, Randall Orndorff, and John Snedden for their thoughtful reviews, which improved the quality of the manuscript.

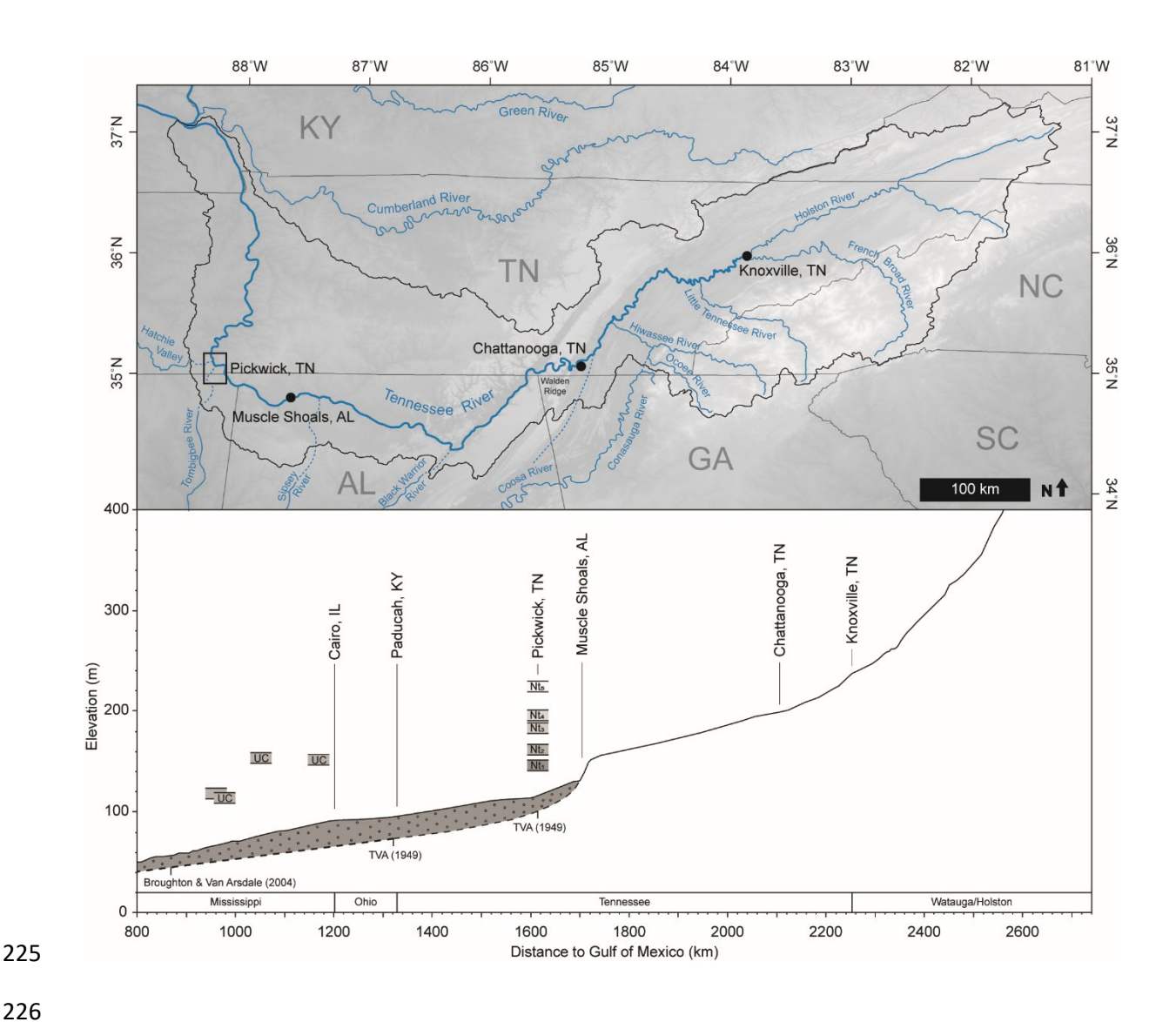


Figure 1. (A) The Tennessee River watershed (black) and major tributaries. Neighboring rivers are also shown. Previously hypothesized paths of the paleo-Tennessee River are indicated by dashed blue lines. (B) Longitudinal profile of the Tennessee River, beginning with the Watauga River in northeastern Tennessee and ending with the Mississippi River. Terraces mapped by Self (2003) are shown at Pickwick, Tennessee. The presence of deep gravels beneath the modern Tennessee River is indicated by gray alluvium; these gravels were interpolated using core data from TVA (1949) and Broughton and Van Arsdale (2004). Locations of the Pliocene Upland Complex are also displayed along the Mississippi River. DEM acquired from The National Map.

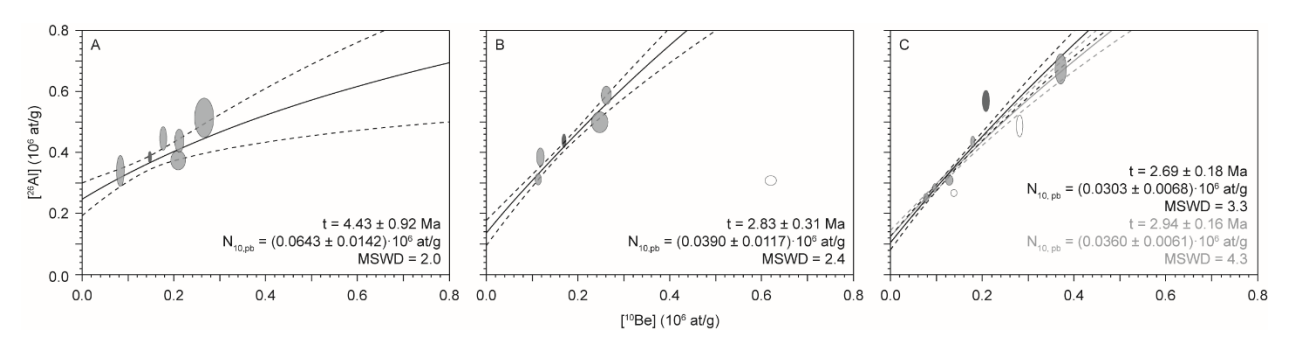


Figure 2. Burial isochrons for the dated terraces. Each ellipse represents a clast (gray) or sand fraction (black) that was used for age calculations. Empty circles indicate reworked samples that were not included in age calculations. Dashed lines represent 1σ uncertainty. (A) The burial isochron for Nt₃ has no reworked clasts and yields an age of 4.43 ± 0.92 Ma (MSWD = 2.0). (B) The burial isochron for Nt₂ has one reworked clast, QFL4-7, that features a significantly lower 26 Al/ 10 Be ratio than other samples. It yields an age of 2.83 ± 0.31 Ma (MSWD = 2.4). (C) The burial isochron for Nt₁ has at least one reworked clast, PW4-4, and yields an age of 2.94 ± 0.16 Ma (MSWD = 4.3) upon removal of the clast (gray isochron line). It is likely that a second clast, PW4-18, is also reworked. Removal of this clast yields a preferred age of 2.69 ± 0.18 Ma (MSWD = 3.3), as shown by the black isochron line.

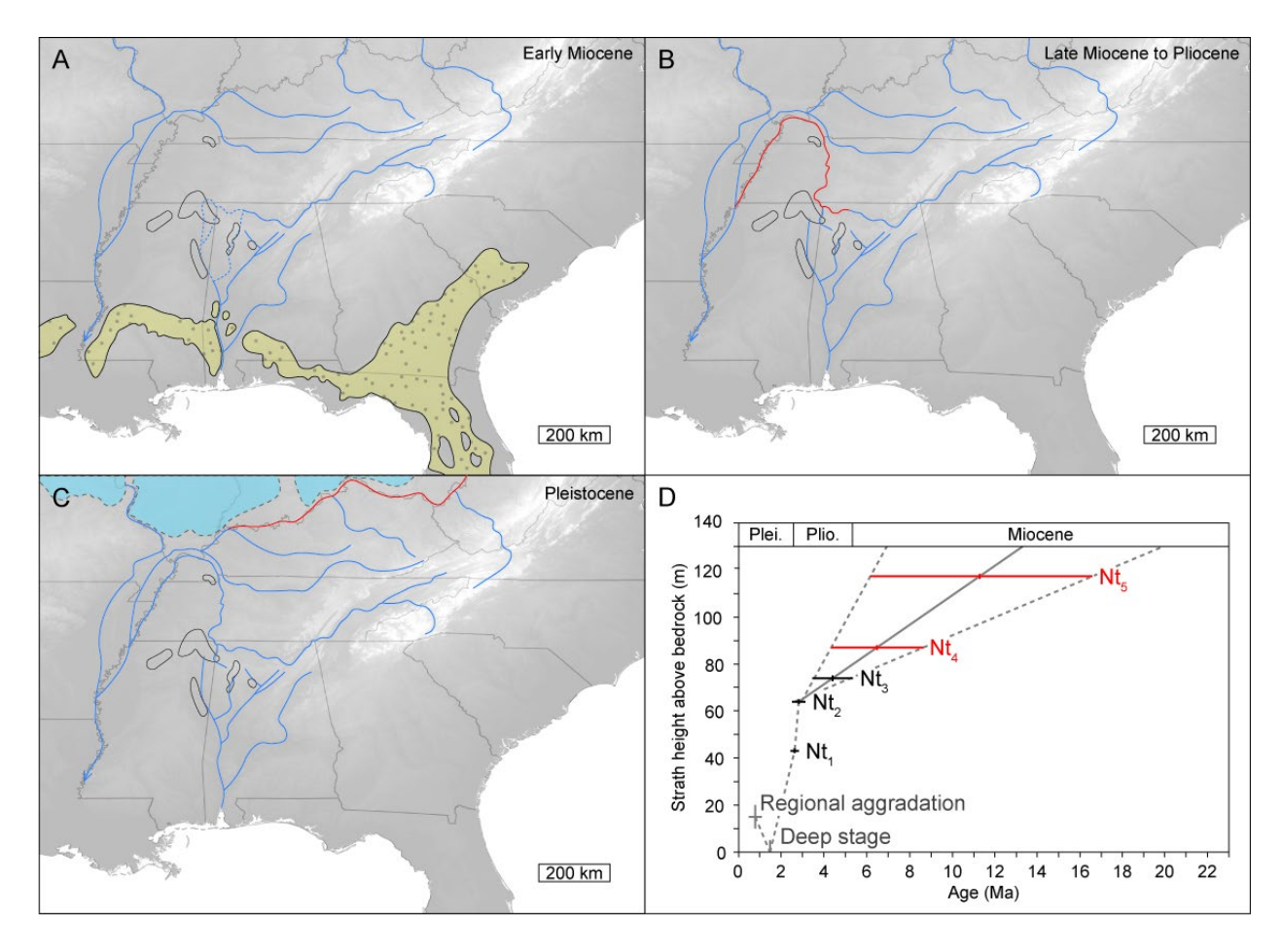


Figure 3. Drainage reconstructions (A-C) and incision history (D) of the Tennessee River since the Early Miocene. Dashed lines indicate potential former connections between the Tennessee and Mobile basins. Major river redirections are highlighted in red. Metamorphic quartz deposits mapped by Mills and Kaye (2001) are outlined in Alabama, Kentucky, Mississippi, and Tennessee. Miocene terrestrial sediments from Isphording and Flowers (1983) are yellow stipple. Laurentide Ice Sheet indicated by blue shading in Pleistocene reconstruction. Inferred ages of undated terraces are indicated in red in Figure 3D; note that terrace level Nt₅ may be as young as latest Miocene. DEM acquired from The National Map.

Table 1

Locations of isochrons and calculated burial ages with analytical uncertainties.

Terrace	Location	Strath (m)	Tread (m)	Elev (m)	m abr	Age (Ma)	MSWD	¹⁰ Be _{post} (10 ⁶ at/g)
Nt_1	35.0908°N, 88.2592°W	139	147	144	48	2.69 ± 0.18	3.3	0.0303 ± 0.0068
Nt_2	35.0201°N, 88.3457°W	154	166	160	64	2.83 ± 0.31	2.4	0.0390 ± 0.0117
Nt ₃	35.0146°N, 88.2442°W	168	179	170	74	4.43 ± 0.92	2.0	0.0643 ± 0.0142

Note. – Terrace level elevations (m abr) refer to site elevation above the bedrock channel of the Tennessee River, while elev (m) refers to elevation of sampled location above sea level.

 $\label{eq:Table 2} \textbf{Sample masses and blank-corrected} \ ^{26}\text{Al}/^{10}\text{Be data}.$

Terrace	Sample	$[^{26}Al] (10^6 \text{ at/g})$	$[^{10}\text{Be}] (10^6 \text{ at/g})$	²⁶ Al/ ¹⁰ Be	Min. age (Ma)	Paleo-E (m/My)
Nt_1	PW4-1	0.2512 ± 0.0150	0.0776 ± 0.0057	3.24 ± 0.31	1.50 ± 0.16	-
Nt_1	PW4-2	0.4352 ± 0.0178	0.1792 ± 0.0047	2.43 ± 0.12	2.04 ± 0.10	-
Nt_1	PW4-3	0.2841 ± 0.0150	0.0970 ± 0.0048	2.93 ± 0.21	1.70 ± 0.14	-
Nt_1	PW4-4	0.2674 ± 0.0116	0.1380 ± 0.0066	1.94 ± 0.12	2.52 ± 0.13	-
Nt_1	PW4-5	0.3102 ± 0.0164	0.1281 ± 0.0076	2.42 ± 0.19	2.08 ± 0.15	-
Nt_1	PW4-13	0.6746 ± 0.0491	0.3704 ± 0.0123	1.82 ± 0.15	2.49 ± 0.14	-
Nt_1	PW4-18	0.4878 ± 0.0357	0.2809 ± 0.0070	1.74 ± 0.13	2.63 ± 0.15	-
Nt_1	PW4-S	0.5699 ± 0.0351	0.2078 ± 0.0077	2.74 ± 0.20	1.78 ± 0.14	5.4 +1.5/-1.1
Nt_2	QF14-1	0.3127 ± 0.0189	0.1131 ± 0.0066	2.76 ± 0.23	1.82 ± 0.15	-
Nt_2	QF14-3	0.5874 ± 0.0292	0.2616 ± 0.0106	2.25 ± 0.14	2.15 ± 0.12	-
Nt_2	QF14-4	0.3850 ± 0.0295	0.1177 ± 0.0088	3.27 ± 0.35	1.48 ± 0.23	-
Nt_2	QFL4-6	0.4990 ± 0.0341	0.2469 ± 0.0183	2.02 ± 0.20	2.39 ± 0.19	-
Nt_2	QFL4-7	0.3077 ± 0.0156	0.6193 ± 0.0123	0.50 ± 0.03	4.51 ± 0.08	-
Nt_2	QFL4-S	0.4389 ± 0.0211	0.1693 ± 0.0040	2.59 ± 0.14	1.91 ± 0.11	$7.0^{+3.0}/_{-2.3}$
Nt ₃	PW1-1	0.4381 ± 0.0381	0.2121 ± 0.0100	2.07 ± 0.20	2.37 ± 0.23	-
Nt_3	PW1-2	0.4462 ± 0.0388	0.1771 ± 0.0077	2.52 ± 0.24	1.98 ± 0.23	-
Nt_3	PW1-3	0.3398 ± 0.0510	0.0840 ± 0.0087	4.05 ± 0.74	1.13 ± 0.34	-
Nt ₃	PW1-4	0.5146 ± 0.0642	0.2666 ± 0.0209	1.93 ± 0.28	2.44 ± 0.29	-
Nt_3	PW1-10	0.3746 ± 0.0313	0.2098 ± 0.0163	1.79 ± 0.20	2.60 ± 0.23	-
Nt ₃	PW1-S	0.3854 ± 0.0179	0.1482 ± 0.0040	2.60 ± 0.14	1.92 ± 0.10	5.5 +7.2/_4.0

 $\label{eq:Table 3} \mbox{Accelerator mass spectrometry data for all measured samples.}$

Sample ID	Mass (g)	Be carrier (µg)	¹⁰ Be/ ⁹ Be (10 ⁻¹⁵)	Total Al (μg)	²⁶ Al/ ²⁷ Al (10 ⁻¹⁵)
PW4-1	16.954	266.9	81.95 ± 3.67	986	194.47 ± 10.74
PW4-2	41.443	268.1	422.86 ± 9.07	1009	802.13 ± 31.93
PW4-3	33.432	268.5	188.89 ± 7.21	874	488.19 ± 24.80
PW4-4	32.207	270.0	254.37 ± 9.94	875	441.76 ± 18.22
PW4-5	22.526	268.4	169.02 ± 7.74	1083	289.72 ± 14.54
WO_BLANK0	-	269.3	8.10 ± 1.77	1010	0.84 ± 0.81
PW1-1	10.83	268.6	129.71 ± 5.60	1211	178.01 ± 13.66
PW1-2	8.202	253.5	87.60 ± 3.28	1077	155.14 ± 11.47
PW1-3	4.511	267.8	22.90 ± 1.78	1254	57.19 ± 6.68
PW1-4	2.962	265.7	46.23 ± 3.07	1106	64.52 ± 5.97
PW4-18	16.135	267.6	255.19 ± 5.86	1270	280.14 ± 18.81
PW1-S	29.716	267.0	248.64 ± 6.23	2743	188.18 ± 8.00
PW4-S	11.906	269.8	138.92 ± 4.69	1307	234.87 ± 12.85
WO_BLANK3	-	270.1	1.72 ± 0.41	1045	2.92 ± 1.84
QFL4-1	18.232	268.0	115.94 ± 6.13	1222	209.11 ± 12.63
QFL4-3	14.893	267.1	219.01 ± 8.24	1319	297.07 ± 14.76
QFL4-4	9.277	267.6	61.83 ± 3.95	1236	129.46 ± 9.91
WO_BLANK10	-	267.0	0.76 ± 0.60	1067	0.00 ± 0.51
PW1-10	5.519	266.3	66.50 ± 4.41	1026	91.51 ± 6.11
PW4-13	13.241	263.2	280.34 ± 8.59	1082	371.12 ± 25.53
QFL4-6	9.861	269.3	136.72 ± 9.37	1344	164.94 ± 10.12
QFL4-7	19.76	262.4	699.33 ± 13.16	1815	150.80 ± 6.77
QFL4-SAND	35.012	268.2	332.18 ± 7.24	3437	200.69 ± 9.21
WO_BLANK11	-	266.3	1.43 ± 0.65	1138	1.13 ± 1.30

Note. – All batches are grouped with their respective Al/Be blanks.

REFERENCES CITED

292

Adams, G. I. 1928. The course of the Tennessee River and the physiography of the southern 293 Appalachian region. J. Geol. 36(6):481-493. 294 Anthony, D. M., and Granger, D. E. 2006. Five million years of Appalachian landscape 295 evolution preserved in cave sediments. Geol. Soc. Am. Spec. Pap. 404:39-50. 296 297 https://doi.org/10.1130/2006.2404(05). Balco, G. 2017. Production rate calculations for cosmic-ray-muon-produced ¹⁰Be and ²⁶Al 298 benchmarked against geological calibration data. Quat. Geochron. 39:150-173. 299 300 https://doi.org/10.1016/j.quageo.2017.02.001 Blum, M. D., Milliken, K. T., Pecha, M. A., Snedden, J. W., Frederick, B. C., and Galloway, W. 301 E. 2017. Detrital-zircon records of Cenomanian, Paleocene, and Oligocene Gulf of 302 Mexico drainage integration and sediment routing: Implications for scales of basin-floor 303 fans. Geosph. 13(6): 2169-2205. https://doi.org/10.1130/GES01410.1 304 Broughton, J. H., and Van Arsdale, R. B. 2004. Surficial geologic map of the Northwest 305 Memphis quadrangle, Shelby County, Tennessee, and Crittenden County, Arkansas. U.S. 306 Geol. Surv. Sci. Inv. Map 2838, scale 1:24,000. https://doi.org/10.3133/sim2838 307 Caffee, M. W., Granger, D. E., Moore, A. K., Odom, W. E., and Ruleman, C. A. 2017. Precise 308 measurement of the ²⁶Al/¹⁰Be production rate ratio from glacial moraine boulders at 309 midlatitudes, USA. 14th Int. Conf. on Accel. Mass Spec., Ottawa, Canada. 310 Chmeleff, J., von Blanckenburg, F., Kossert, K., and Jakob, D. 2010. Determination of the ¹⁰Be 311 half-life by multicollector ICP-MS and liquid scintillation counting. Nucl. Instruments 312 Methods Phys. Res. B: Beam Interact. with Mater. Atoms 263(2): 192-199. 313 314 https://doi.org/10.1016/j.nimb.2009.09.012

Gallen, S. F. 2018. Lithologic controls on landscape dynamics and aquatic species evolution in 315 post-orogenic mountains. Earth Planet. Sci. Lett. 493: 150-160. 316 https://doi.org/10.1016/j.epsl.2018.04.029 317 Gallen, S. F., Wegmann, K. W., and Bohnenstiehl, D. R. 2013. Miocene rejuvenation of 318 topographic relief in the southern Appalachians. GSA Today 23(2): 4-10. 319 320 https://doi.org/10.1130/GSATG163A.1 Galloway, W. E., Whiteaker, T. L., and Ganey-Curry, P. 2011. History of Cenozoic North 321 American drainage basin evolution, sediment yield, and accumulation in the Gulf of 322 Mexico basin. Geosphere 7(4): 938-973. https://doi.org/10.1130/GES00647.1 323 Granger, D. E., Fabel, D., and Palmer, A. N. 2001. Pliocene-Pleistocene incision of the Green 324 River, Kentucky, determined from radioactive decay of cosmogenic ²⁶Al and ¹⁰Be in 325 Mammoth Cave sediments. Geol. Soc. of Am. Bulletin 113(7): 825-836. 326 https://doi.org/10.1130/0016-7606(2001)113<0825:PPIOTG>2.0.CO;2 327 Hayes, C. W., Campbell, M. R. 1894. Geomorphology of the southern Appalachians. Nat. Geog. 328 Soc. 6: 63-126. 329 Hoagstrom, C. W., Ung, V., and Taylor, K. 2014. Miocene rivers and taxon cycles clarify the 330 331 comparative biogeography of North American highland fishes. J. Biogeog. 41(4): 644-658, https://doi.org/10.1111/jbi.12244 332 333 Isphording, W. C., and Flowers, G. C. 1983. Differentiation of Unfossiliferous Clastic 334 Sediments: Solutions from the Southern Portion of the Alabama-Mississippi Coastal Plain. Tulane Stud. Geol. Paleo. 17(3): 59-83. 335 Johnson, D. W. 1905. The Tertiary history of the Tennessee River. J. Geol. 13(3): 194-231. 336 337 Korschinek, G., Bergmaier, A., Faestermann, T., Gerstmann, U.C., Knie, K., Rugel, G., Wallner,

338	A., Dillmann, I., Dollinger, G., Von Gostomski, C.L., Kossert, K. 2010. A new value for
339	the half-life of ¹⁰ Be by heavy-ion elastic recoil detection and liquid scintillation counting
340	Nucl. Instruments Methods Phys. Res. B: Beam Interact. with Mater. Atoms 268: 187-
341	191. https://doi.org/10.1016/j.nimb.2009.09.020.
342	Kozak, K. H., Russell, A. B., Larson, A. 2006. Gene lineages and eastern North American
343	palaeodrainage basins: phylogeography and speciation in salamanders of the Eurycea
344	bislineata species complex. Molec. Ecol. 15: 191-207. https://doi.org/10.1111/j.1365-
345	294X.2005.02757.x
346	Mayden, R. L. 1988. Vicariance biogeography, parsimony, and evolution in North American
347	freshwater fishes. Sys. Biol. 37(4): 329-355. https://doi.org/10.1093/sysbio/37.4.329
348	Milici, R. 1968. Mesozoic and Cenozoic Physiographic Development of the Lower Tennessee
349	River: In Terms of the Dynamic Equilibrium Concept. J. Geol. 76(4): 472–479.
350	https://doi.org/10.1086/627345
351	Mills, H. H., and Kaye, J. M. 2001. Drainage history of the Tennessee River: review and new
352	metamorphic quartz gravel locations. SE Geol. 40(2): 75-97.
353	Mills, H. H., Sumners, D. N., Hart, E. A., and Li, P. 2005. Distribution of high-level alluvial
354	deposits in the Valley and Ridge of Polk County, southeastern Tennessee: implications
355	for river history and drainage evolution. SE Geol. 44: 37-44.
356	Near, T. J., and Keck, B. P. 2005. Dispersal, vicariance, and timing of diversification in
357	Nothonotus darters. Molec. Ecol. 14(11): 3485-3496. https://doi.org/10.1111/j.1365-
358	294X.2005.02671.x
359	Nishiizumi, K. 2004. Preparation of ²⁶ Al AMS standards. Nucl. Instruments Methods Phys. Res
360	B: Beam Interact. with Mater. Atoms 233: 388-392.

- Odom, W. E., Hofmann, F., Van Arsdale, R. B., Granger, D. E. 2020. New ²⁶Al/¹⁰Be and (U-
- Th)/He constraints on the age of the Upland Complex, central Mississippi River Valley.
- Geomorph. 371: 1-9. https://doi.org/10.1016/j.geomorph.2020.107448
- Parks, W. S. 1992. Four levels of terrace deposits and remnants of high-level fluvial deposits in
- the Hatchie River Valley, Hebron area, Hardeman County, Tennessee. Miss. Geol. 13(4):
- 366 63-70.
- Parks, W. S., and Russell, E. E. 1975. Geologic map showing upper Cretaceous, Paleocene, and
- lower and middle Eocene units and distribution of younger fluvial deposits in western
- Tennessee. U.S. Geol. Surv. Misc. Inv. Series Map I-916, scale 1:250,000.
- Persons, A. K. 2010. Geological and ichthyological investigations into palaeodrainage
- hypothesis for the Tennessee River [Ph.D. thesis]. Univ. of S. Miss. 158.
- Potter, P. E. 1955. The petrology and origin of the Lafayette gravel, part 2: geomorphic history.
- 373 J. Geol., v. 63(2): 115-132.
- Russell, E. E., and Schmitz, D. W. 2003. Implications of comparisons of Tennessee with
- Tombigbee River depositional systems. Geol. Soc. of Am. SE Sect. Abstr. with Progr. 35:
- 376 70.
- 377 Self, R. P. 2003. The Cretaceous to late Tertiary gravel deposits in the western Tennessee River
- valley. St. Tenn. Dept. Env. Conserv. Rep. Inv. 51: 1-14.
- 379 Snedden, J.W., Galloway, W.E., Milliken, K.T., Xu, J., Whiteaker, T., and Blum, M.D., 2018,
- Validation of empirical source-to-sink scaling relationships in a continental-scale system:
- The Gulf of Mexico basin Cenozoic record: Geosphere, v. 14, no. 2, p. 1-17,
- doi:10.1130/GES01452.1.
- Snedden, J. W., and W. E. Galloway, 2019, The Gulf of Mexico Sedimentary Basin:

384	Depositional Evolution and Practical Applications: Cambridge, United Kingdom,
385	Cambridge University Press, 344 p., doi:10.1017/9781108292795
386	Starnes, W. C., and Etnier, D. A. 1986. Drainage evolution and fish biogeography of the
387	Tennessee and Cumberland rivers drainage realm. Zoography N. Am. freshwater fishes,
388	p. 325-361.
389	Tennessee Valley Authority. 1949. Geology and foundation treatment. Tenn. Vall. Auth. Proj.
390	Tech. Rep. 22: 1-548.
391	Wittmann, H., von Blanckenburg, F., Maurice, L., Guyot, J., Filizola, N., Kubik, P. W. 2011.
392	Sediment production and delivery in the Amazon River basin quantified by in situ-
393	produced cosmogenic nuclides and recent river loads. GSA Bull. 123(5/6): 934-950.
394	https://doi.org/10.1130/B30317.1
395	Xu, J., Snedden, J. W., Stockli, D. F., Fulthorpe, C. S., and Galloway, W. E. 2017. Early
396	Miocene continental-scale sediment supply to the Gulf of Mexico Basin based on detrital
397	zircon analysis. GSA Bull. 129(1-2): 3-22. https://doi.org/10.1130/B31465.1